

# BEAM INSTRUMENTATION FOR FUTURE HIGH INTENSE HADRON ACCELERATORS AT FERMILAB\*

M. Wendt<sup>#</sup>, M. Hu, G. Tassotto, R. Thurman-Keup, V. Scarpine, S. Shin, J. Zagel, Fermilab, Batavia, IL 60510, U.S.A.

## Abstract

High intensity hadron beams of up to 2 MW beam power are a key element of new proposed experimental facilities at Fermilab. Project X, which includes a SCRF 8 GeV H<sup>-</sup> linac, will be the centerpiece of future HEP activities in the neutrino sector. After a short overview of this, and other proposed projects, we present the current status of the beam instrumentation activities at Fermilab with a few examples. With upgrades and improvements they can meet the requirements of the new beam facilities, however design and development of new instruments is needed, as shown by the prototype and conceptual examples in the last section.

## INTRODUCTION

In September 2010 Fermilab plans to finish the Run II p/pbar collider HEP physics run, and its primary use of the 980 GeV/c Tevatron. Fermilab will continue neutrino oscillation physics, and related HEP programs at the high-intensity hadron beam frontier, using the NuMI beam-line, achieving today a beam power of ~300kW, utilizing  $4 \times 10^{13}$  protons @ 120 GeV from the Main Injector (MI) at a 2.2 sec cycle time (Fig. 1). Other accelerator based activities include an 8 GeV beam-line to the MiniBooNE, MicroBooNE experiments, and 150 GeV beam-lines through Switchyard, e.g. to dedicated detector experiments.

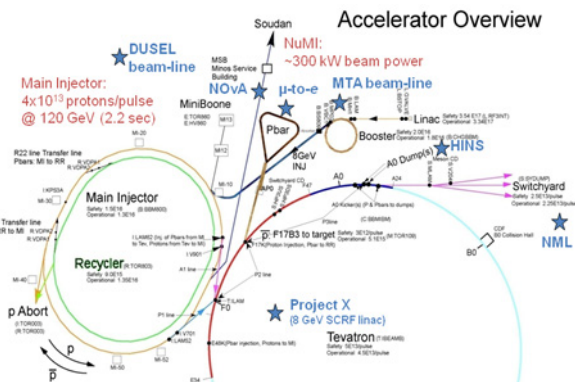


Figure 1: Accelerator complex and future activities at Fermilab.

Beside NuMI, a series of new projects, experiments and R&D activities has been started to ensure an exciting accelerator based research program after the shutdown of the Tevatron.

\* This work was supported by Fermi National Accelerator Laboratory, operated by Fermi Research Alliance, LLC under contract No. DE-AC02-07CH11359 with the United States Department of Energy  
<sup>#</sup>manfred@fnal.gov

## MTA beam-line

This 400 MeV beam-line is completely assembled and located at the end of the H<sup>-</sup> Linac, and will be commissioned with beam by end of 2008. It is part of the Muon Collider task force, and will serve as a test bed to study basic techniques and components for a muon ionization cooling system.

## NOvA, ANU (Accelerator and NuMI Upgrades)

The NOvA  $\nu_\mu \rightarrow \nu_e$  oscillation experiment, currently at DOE approval level CD-3, is based on an upgrade of the Fermilab accelerators (ANU), to provide 700 kW beam power to the NuMI beam-line. This upgrade will take place after the Tevatron Run II is finalized, so that the Recycler can be used as proton storage ring for a more efficient stacking of protons to the Main Injector. The upgrade includes new injection and extraction beam-lines between Recycler and Main Injector, new RF systems and cavities, injection/extraction elements, and of course new beam diagnostics.

## $\mu$ -to- $e$ Conversion

This new “beyond the standard model” experiment is in an early conceptual design phase (pre CD-0). It tracks backscattered muons from an 8 GeV proton production target to observe a rare muon to electron conversion. The project will use an 8 GeV single proton bunch ( $1.8 \times 10^{12}$ , 100 nsec long, 1.6 usec revolution time) from the (to be modified) Accumulator/Debuncher complex. Several crucial beam diagnostics challenges go along with this setup, including a very sensitive beam gap monitor (resolution  $10^{-9}$ ), and a mission critical slow resonant extraction system. New instrumentations systems have to be developed to characterize the muon beam parameter. At a later stage the forward scattered shower may be used for muon cooling experiments, which would require sensitive diagnostics to measure low intense ( $10^7$ )  $\mu$ -beams.

## NML SCRF Beam Test Facility

A superconducting RF beam test facility is under construction at the NML building, to test SCRF cryomodules, and the related RF and cryogenic infrastructure under realistic beam conditions. Even though this facility will be operated with an electron beam, it will facilitate a Project X like beam structure, thus requiring Project X equivalent beam instrumentation.

### HINS

The High Intensity Neutrino Source (HINS) is a SCRF-based H<sup>-</sup> front-end R&D effort for Project X, located at the Muon detector building [1]. Proton beams at 2.5 MeV are expected in early 2009, H<sup>-</sup> beams sometime later that year. While the focus is on RF systems and accelerating structures (normal and superconducting), the characterization of the beam parameters, including beam halo, longitudinal tails and beam losses are crucial as well. HINS will be the major hadron beam R&D facility at Fermilab to test new beam diagnostics.

### DUSEL

A Deep Underground Science and Engineering Laboratory (DUSEL) is planned to be located at the Homestake Mine site (South Dakota) for very-long-baseline neutrino experiments. It requires a new 120 GeV beam-line to deliver from 700 kW (ANU) to 2 MW (Project X) beam power on the target. Similar to the NuMI beam-line, beam loss detection, machine protection, beam orbit, etc. are key diagnostic elements for this project.

### Project X

Project X is Fermilab's main enterprise towards accelerator based HEP at the high-intensity beam frontier. It will replace the current H<sup>-</sup> Linac and proton Booster synchrotron, supplying an 8 GeV, 360 kW H<sup>-</sup> beam for multiturn stripping into Recycler and Main Injector [2]. Also the H<sup>-</sup> transport beam-line [3] and the modifications at the Main Injector, Recycler, and target beam-lines are defined within Project X. Most of the required beam instrumentation can be developed and tested at HINS or NML, however a high intensity 8 GeV H<sup>-</sup> beam will give additional challenges, e.g. detection system of the laser wire beam profile monitor.

All these ongoing and future high-intensity hadron beam accelerator projects require state-of-the-art beam instrumentation and diagnostics. Emphasis will be on non-invasive detectors and characterization of beam profiles / emittances, as well as beam halo measurements to identify (and cure) beam blow-up and losses (emittance preservation). Beam loss monitoring and machine protection are crucial for the day-to-day operation and need to be made fail safe.

## STATUS OF HADRON BEAM DIAGNOSTICS AT FERMILAB

To meet the challenging requirements in terms of beam instrumentation for Project X and the other planned facilities, let us summarize the current status of some crucial beam diagnostics installations at Fermilab.

### Flying Wire Beam Profile Monitor

The Main Injector Flying Wires use a 33μm carbon filament and are flown for every proton and antiproton bunch transfer to the Tevatron during shot setup (Fig. 2). The protons are on the order of 3e11 particles per bunch.

At this intensity, the wires are flown at 6 meters per second, and make 2 passes through the beam. Each pass takes about 5 ms, (about 450 beam revolutions) with 40 ms between passes.

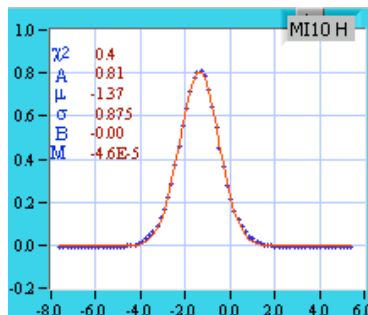


Figure 2: A typical MI fly at 150 GeV Tevatron injection energy. Amplitude, mean position, sigma (Gaussian), and baseline are displayed along with the precision of the fit.

Experience has shown that NuMI beam energy and intensities (4e13 at 120 GeV) are sufficient to destroy the Main Injector wires flying at this speed. A calculation of the peak temperature of the wire based on restricted energy deposition (about 1.35 MeV\*cm<sup>2</sup>/g for this wire diameter, at 120 GeV), radiative cooling between the passes, and the best knowledge of the local amplitude function, resulted in a temperature of about 500 Kelvin in excess of the melting point after the second pass through the beam. Solutions for this problem include changing the local amplitude function to increase beam spot size (not likely due to lattice considerations), using wires of smaller diameters to decrease energy deposition and increase radiative cooling efficiency, or increasing the wire speed through the beam. Applications of this technique for future high brightness beam monitoring are under consideration.

### Ionization Profile Monitor (IPM)

The Main Injector Ionization Profile Monitors are of 2 different types. The Original Main Ring IPM's are electrostatic devices that are set to collect ions created when protons strike residual gas molecules. They have a positive 30 kV clearing field to move the ions created toward a pair of Micro-Channel Plates (MCP). The output of the MCP's are collected on copper strips spaced at 0.5 mm pitch and amplified with a 60 db preamp with a 300 kHz roll-off. These signals are digitized once per revolution in the Main Injector (11.1 μsec) to create one complete profile per revolution. Up to 65,535 turns can be captured in a single measurement. At 8 GeV, Main Injector injection energy, these devices give a close approximation of the beam profile. However at extraction energy of 150 GeV there is a significant spread of the ions due to the space charge of the beam. To counteract this effect, we designed a second generation magnetic system referred to as the Mark-II. The Mark-II uses a magnetic field to contain the electrons liberated in the collisions to a small radius consistent with the pick-up strip spacing. A smaller E-Field of negative 10 kV then accelerates the electrons toward the MCP's.

A comparison of 8 GeV Flying Wire and IPM measurements from the Main Injector was published in [4]. For the IPM systems a higher intensity beam will

provide a better signal, however with better vacuum the signal decreases. In the Tevatron this has been detailed in [5], which includes a comparison of IPM to Flying Wire measurements.

### Secondary Emission Monitors (SEM) for High Intensity Beam Profiling at NuMI

For NuMI, the beam-line which presently runs the highest intensity beams at Fermilab (see Table 1), Secondary Emission Monitors, (SEM) - also called multiwires - are used as beam profile monitors. Because of the beam loss that SEMs generate they are typically only used during tuning periods except for the target SEM which is always in the beam.

Table 1: Beam parameters of the NuMI beam-line

NuMI beam parameters	
Energy	120 GeV
Beam intensity	4e13 protons/spill
Beam power	up to 350 kW
Spill time	8.56 $\mu$ sec
Cycle time	2.2 sec

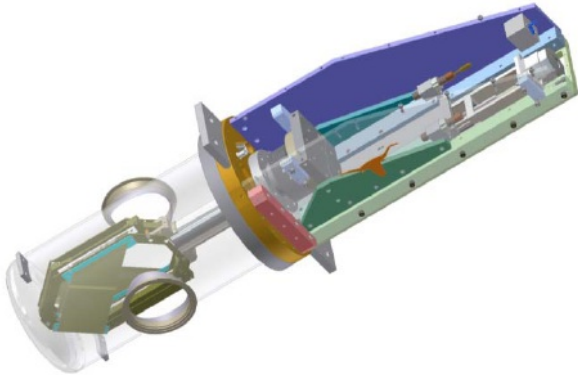


Figure 3: UTA SEM.

Two types of SEMs have been built to profile the beam:

1. University of Texas (UTA):

These SEMs (except for the target SEM) have an x, y signal plane. They have 44 Ti strips each which are 5  $\mu$ m thick, 0.15 mm width, and have a pitch of 1 mm. The wires in the target SEM have a pitch of 0.5 mm. They also have a Ti bias foil 2.5  $\mu$ m thick. Figure 3 shows a picture of a UTA SEM [6].

2. FNAL SEM:

One detector (PM118) has been built and tested having x and y planes made with 48 Ti strips each which are 12.5  $\mu$ m thick, 0.20 mm width at a pitch of 1 mm. There is no bias foil. A prototype SEM is being built having 25  $\mu$ m Ti wires at a pitch of 1 mm that will be installed in the beamline during the next shutdown. Fig. 4 shows a wire plane assembly for PM118.

Calculations to estimate beam losses have been done both at UTA and FNAL. For a typical UTA SEM it was

estimated to be  $2.6 \times 10^{-6}$  interaction lengths. For PM118, presently under test, the estimate is for  $1.78 \times 10^{-5}$  interaction lengths and for the newly built SEM having 25  $\mu$ m Ti wires the estimate is  $3.56 \times 10^{-6}$  interaction lengths. This will enable an operator to set a SEM IN/OUT of the beam without tripping the radiation detector set at 5 Rad/sec.

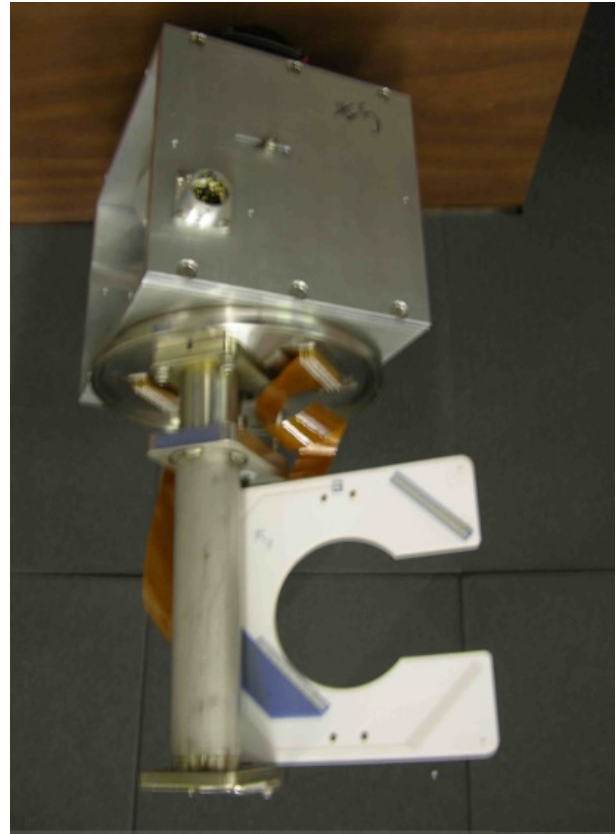


Figure 4: FNAL SEM.

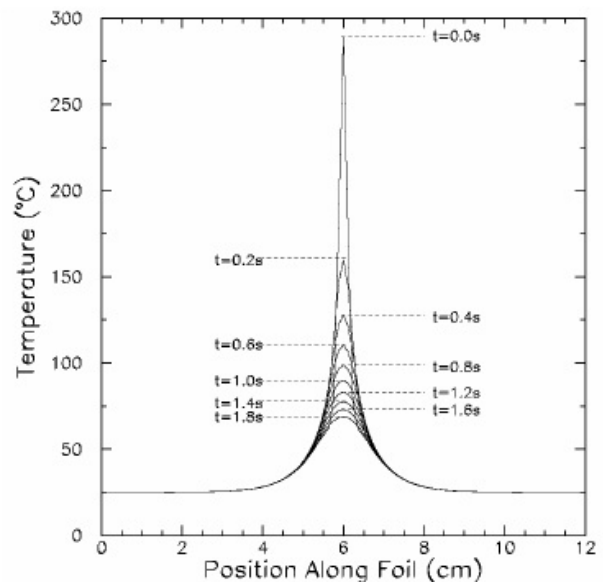


Figure 5: Temperature effects on a multiwire SEM.

UTA simulated the temperature rise of various materials (see report NuMI-B-926). For a 5  $\mu$ m thick Ti foil the

temperature increase is almost 300 C (Fig. 5). For a 25 μm Ti wire the expected temperature rise will cause wire failure at  $1.64 \times 10^{14}$  protons. It is possible to increase the beam intensity by selecting other materials, particularly carbon which has a high melting temperature (3500 C.), low density,  $2.2 \text{ g/cm}^3$ , (versus  $4.54 \text{ g/cm}^3$  for Ti) and high emissivity (8 times greater than Ti). This will enable carbon filaments to survive much higher intensities while generating manageable beam losses, and gives confidence for the upgrade to 700 kW beam power.

**Beam Profile Monitors based on Optical Transition Radiation (OTR)**

Optical transition radiation is generated when a charged particle transits the interface of two media with different dielectric constants (e.g., vacuum to dielectric or vice versa) [7], [8]. The expression for the single-particle spectral angular distribution of the number of photons,  $N$ , per unit frequency ( $d\omega$ ) and solid angle ( $d\Omega$ ) is given by [8], [9]:

$$\frac{d^2N}{d\omega d\Omega} = \frac{2e^2}{\pi h c \omega} \frac{(\theta_x^2 + \theta_y^2)}{(\gamma^{-2} + \theta_x^2 + \theta_y^2)^2} \quad (1)$$

where  $e$  is the electron charge,  $h$  is Planck’s constant,  $c$  is the speed of light,  $\gamma$  is the Lorentz factor of the charged particle, and  $\theta_x$  and  $\theta_y$  are the angles from the OTR emission axis. For the forward OTR this axis is the same as the particle beam while for the backward OTR this axis is the specular reflection axis. In addition, the intensity of the backward OTR is proportional to the reflectivity of the surface. This expression shows that the angular distribution is maximum at  $\theta \sim 1/\gamma$ . Figure 6 shows the angular distribution of OTR

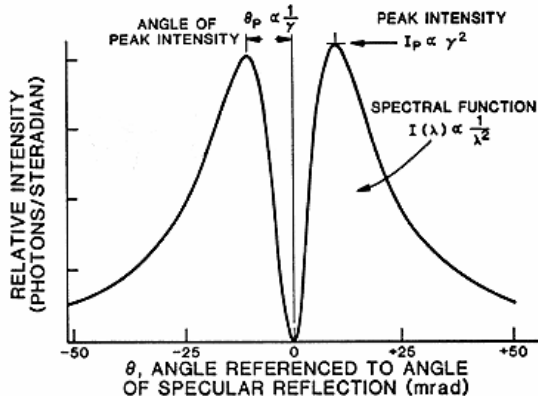


Figure 6: Angular distribution of OTR emission.

OTR detectors have been used extensively to measure transverse beam shape in electron accelerators. Recently, CERN incorporated OTR detectors in various transfer lines to measure proton bunches used for operation of the LHC [7]. As part of the Run II collider plan and the NuMI neutrino program, a series of OTR detectors were designed, constructed and installed in various beam-lines at Fermilab. Previous near-field OTR images, from other Fermilab beam-lines, of lower-intensity 120 GeV and 150 GeV protons with larger transverse beam size have been

presented [11], [12], [13]. An OTR detector has been installed in the Fermilab NuMI proton beamline, which operates at beam powers of up to ~350 kW, to obtain real-time, spill-by-spill beam profiles for neutrino production. NuMI OTR images of 120 GeV protons for beam intensities up to  $4.1 \times 10^{13}$  at a spill rate of 0.5 Hz and small transverse beam size of ~1 mm (sigma) have been measured [14]. A detailed description of the OTR detector can be found in reference [15].

Figure 7 shows OTR images for bunch intensities of  $\sim 2.4 \times 10^{13}$  and  $\sim 4.1 \times 10^{13}$  protons. This figure also shows the beam projections with Gaussian fits. The images show the increase in beam size with increase in beam intensity. The images also show an increase in the beam ellipticity with higher intensities. This shows the advantage of a two-dimensional beam shape monitor, such as an OTR detector, over other standard one-dimensional profile monitors.

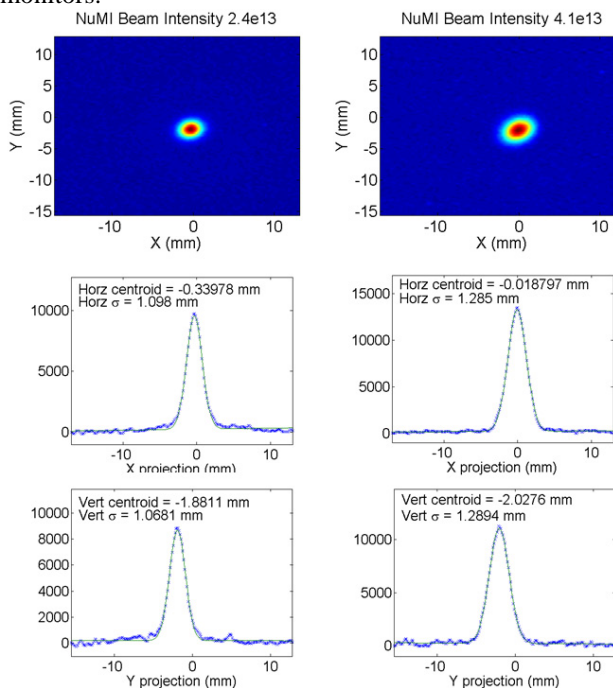


Figure 7: NuMI OTR beam images and horizontal and vertical projections with Gaussian fits for  $2.4 \times 10^{13}$  and  $4.1 \times 10^{13}$  protons per bunch Accelerator complex and future activities at Fermilab.

The choice of a 6 micron thick, aluminized Kapton foil for the NuMI OTR was made to minimize the scatter of the NuMI beam. Issues of foil lifetime at this high beam intensity are not well understood but it was assumed that the foil would change over time. Figure 8 shows a comparison of the measured horizontal beam  $\sigma$  from an adjacent SEM monitor and the OTR detector over a period of 80 days. This corresponds to  $\sim 6.5 \times 10^{19}$  protons through the Kapton foil. One can see from the figure that value of  $\sigma$  for the OTR detector is slowly diverging from the value from the SEM monitor indicating possible aging of the Kapton foil. Comparison of the primary OTR foil to a unused secondary foil clearly indicates that the Kapton foil is changing.

The extended use of OTR detectors as potential profile monitors for future intense proton beams will primarily depend on the survivability of the OTR foil. However, non-continuous use of OTR detectors in an intense proton beam-line is an option for transverse profile measurements.

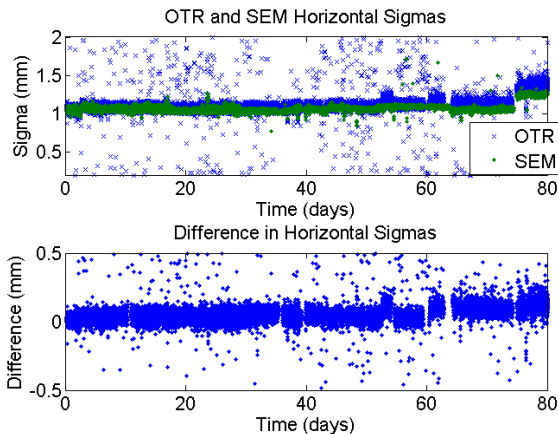


Figure 8: Comparison of the horizontal  $\sigma$  between the SEM monitor and the OTR detector over time.

### Beam Loss Monitors

An ion chamber style detector is used at the majority of locations throughout the Fermilab accelerators for local beam loss detection [16]. Long, gas-filled Heliac coaxial cables, based on the same ionization principle, are used as total loss monitors (TLM), integrating over long beam-line sections. For low-energy beams, plastic scintillators with high gain PMTs are used as the detection element.

### Ion Chamber Detector

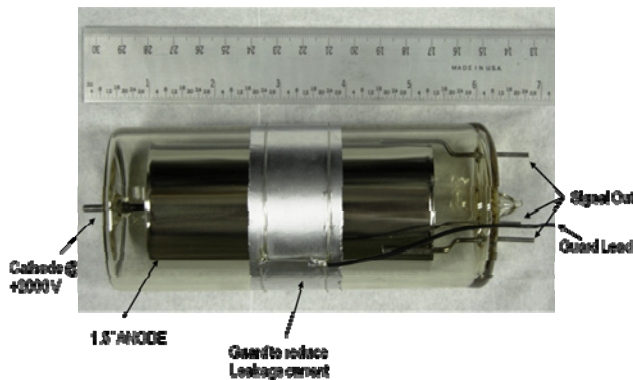


Figure 9: Ion chamber beam loss detector.

Figure 9 shows the argon-filled, cylindrical glass ion chamber with nickel electrodes. The design was optimized for radiation hardness, high gain, response time, size, and costs. Table 2 summarizes some specifications of this detector type.

Table 2: Ion chamber beam loss detector specifications

Specifications	
Materials	Glass, Nickel
Volume	110 ccm argon gas at 1 atm
Calibration	70 nC / rad
Response time	1-2 $\mu$ sec
Leakage current	<10 pA
Operating Range	1 mrad – 100 rad

### Gas-Filled Coaxial Cable TLM

This total loss monitor is a very simple construction, based on 7/8" air dielectric *Heliac* coaxial cables, flowed with ArCO<sub>2</sub>. It requires a continuing gas circulation because the outgassing of the PE dielectric stand-offs would poison the gas and change the detector characteristics.

### Plastic Scintillator / PMT

Scintillator materials used are NE-102 (made from Polyvinyltoluene) or – preferred for radiation hardness – Polyimide. The light is amplified with a high gain photomultiplier tube (PMT), such that this beam loss detector can be applied at low energy beam-lines.

Practical issues during long term operation of these beam loss detectors, and the related hardware in the tunnel (cables, connectors, electronics) are in non radiation tolerant materials, such as PTFE (Teflon) as connector dielectrics, stand-off insulators, etc.

### Other Beam Instrumentation

Beside the mentioned beam diagnostics for transverse beam profile and beam loss monitoring, the Fermilab accelerator chain is equipped with myriad general purpose and dedicated beam instrumentation systems, e.g.:

- Beam Position Monitors (BPM)**  
 Stripline or split-plate pickup stations, digital signal processing based on Echotek digital receiver technology.
- Longitudinal Beam Profile Monitors**  
 Based on broadband (up to 10 GHz BW) wall current monitors, fast oscilloscopes, and data processing for bunch length, beam phase and energy, etc.
- Beam Current Monitoring**  
 Based on toroidal transformers and DCCTs.
- Special Diagnostics**  
 BPM-based beam-line tuning systems for injection, abort gap monitoring based on synchrotron light, single bunch tune meter, Schottky monitor systems at microwave frequencies (tune, chromaticity), etc.

### DIAGNOSTICS DEVELOPEMENTS FOR FUTURE BEAM FACILITIES

Some of the challenges for high-intense hadron beam instrumentation in the upcoming projects at Fermilab (see Introduction) are:

- Transverse beam size measurements at very high beam intensities, e.g. using
  - Very thin physical wires?
  - Laser wire (only for H<sup>-</sup> beams)
  - Ionization profile monitors (IPM)
  - Electron-beam wire monitor
- Beam halo characterization (crawling wire, laser wire, vibrating wire, screen monitors (OTR) with micro-mirrors, etc.)
- Resonant extraction feedback systems
- Beam gap instrumentation with high dynamic rang (1:10<sup>9</sup>).
- Diagnostics for low energy (keV to few MeV) beams (BPMs, emittance).
- Beam monitors in cryogenic environments
  - BPM pickup (button, resonant cavity)
  - Use of HOM coupler signals as beam pickup.
- Machine protection systems
  - BLM-based interlock systems with minimal response time (5-10 μsec).
  - BPM-based orbit verification systems, with automatic gain correction.

A few instrumentation projects have been started, most focused to meet HINS / Projects X requirements.

#### Laser Wire Profile Monitor

Measurements of the transverse profiles of H<sup>-</sup> beams, using laser induced photodetachment, have been investigated by several groups including BNL [17] and SNS [18] [19]. Laser induced photodetachment has also been studied as a longitudinal profile monitor [18] [20]. A focused laser, of the appropriate wavelength, is scanned, either transversely or longitudinally, across the H<sup>-</sup> beam liberating electrons. The longitudinal or transverse beam profiles can be determined by either measuring, as a function of laser position, the liberated electrons or the change of H<sup>-</sup> beam current. The basis of these measurements is the threshold for photodetachment of an electron, which is about 0.75 eV with a cross section of ~4 x 10<sup>-17</sup> cm<sup>2</sup> for photons of ~1.5 eV in the H<sup>-</sup> rest frame. Figure 10 show the photodetachment cross section versus photon energy [21]. The fraction of H<sup>-</sup> undergoing photodetachment, *f*, is given by

$$f = 1 - e^{-\sigma(E)Ft} \tag{2}$$

where  $\sigma(E)$  is the photodetachment cross section, *F* is the laser photon flux and *t* is the flight time of the H<sup>-</sup> beam through the laser [17].

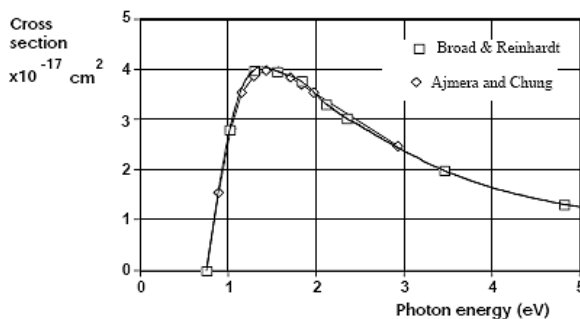


Figure 10: Photodetachment cross section of H<sup>-</sup> vs photon energy in H<sup>-</sup> rest frame [21].



Figure 11: Initial transverse beam profile measurements at BNL of 750 keV H<sup>-</sup>.

BNL has developed a prototype laser wire transverse profile monitor for Fermilab as part of the High Intensity Neutrino Source (HINS) project. The monitor utilizes a Q-switched, Nd:YAG laser with an energy of 50 mJ per pulse. The monitor can transversely scan both horizontally and vertically across the beam utilizing fast rotating mirrors. The liberated electrons are collected by a Faraday cup as a function of laser position. This monitor has successfully measured 750 keV H<sup>-</sup> beam profiles at BNL. Figure 11 shows an initial profile measurement taken at BNL.

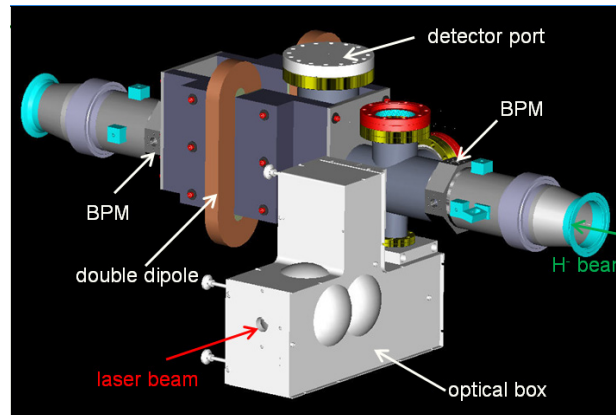


Figure 12: Drawing of laser wire profile monitor to measure 400 MeV H<sup>-</sup> beam entering the Fermilab booster.

This BNL profile monitor is intended to measure HINS H<sup>-</sup> beam from 2.5 MeV up to 66 MeV. Initially, to develop operational experience, this monitor will be

installed at the entrance of the Fermilab booster and measure 400 MeV H<sup>-</sup> beam profiles. The liberated electrons will be transported by the first half of a double dipole magnet to a scintillator and PMT detector instead of Faraday cup. The second half of the double dipole magnet will operate to compensate for any deflection of the primary H<sup>-</sup> beam by the first half. Figure 12 shows a drawing of the laser wire profile monitor assembly intended for installation.

For both the HINS and the proposed Project-X accelerators, non-intercepting profile monitors are strongly preferred, if not required. For these accelerators, Fermilab plans on utilizing laser wire profile monitors as prime transverse profile monitors for H<sup>-</sup> beams from a few MeV up to 8 GeV. In addition, laser wires will also be developed to measure longitudinal profiles for these accelerators. To operate over this range of beam energies, investigation of various electron collection schemes is required. A future goal of complete profile measurements in a single macro-pulse will require development of new technologies, such as high-power CW lasers and femtosecond fiber lasers.

### Resonant Cavity Beam Position Monitor

Above a beam energy of ~400 MeV Project X is based on superconducting 1.3 GHz RF accelerating structures, applying the TESLA/ILC technology. A string of 40 cryomodules, each housing several 9-cell cavities, as well as one or more SC quadrupole magnets and correctors, will boost the beam energy to 8 GeV. The beam diagnostics along this cryogenic string will likely be limited to BPMs located at the quadrupoles, as of the SCRF related requirements:

- Ultra-high vacuum (<1e-9 Torr)
- 2 K cryogenic temperature certification
- Clean-room class 100 certification
- No moving parts!

A cylindrical “pillbox” having conductive (metal) wall dimensions of radius  $R$  and length  $l$  resonates at eigenfrequencies:

$$f_{mnp} = \frac{1}{2\pi\sqrt{\mu_0\epsilon_0}} \sqrt{\left(\frac{j_{mn}}{R}\right)^2 + \left(\frac{p\pi}{l}\right)^2} \quad (3)$$

This resonator can be utilized as a passive, beam driven cavity BPM by assembling it into the vacuum beam pipe. A subset of these eigenmodes is excited by the beam, for use as a BPM the lowest transverse-magnetic dipole mode  $TM_{110}$  is of interest. The

$$E_z = C J_1\left(\frac{j_{11}r}{R}\right) \cos\phi e^{i\alpha z} \quad (4)$$

field component couples to the beam, with almost linear dependence to the beams displacement  $r$ , and beam intensity (hidden in the constant  $C$ ). Most of the “unwanted” modes are absorbed by the beam pipe (acting as a waveguide shunt), or need to be filtered. This is particularly important for the  $TM_{010}$  monopole mode, since  $f_{010} < f_{110}$ , to avoid a common mode signal

contribution at  $f_{110}$  due to the finite Q-factor of the resonances.

In the framework of the GDE ILC collaboration efforts a CM-free cold L-Band cavity BPM is under construction[22] (Fig. 13), to fulfill the ILC needs, i.e. single bunch beam position measurement (at ~300 ns bunch spacing) utilizing a moderate Q-factor (600-700), <1  $\mu$ m resolution, 78 mm beam pipe aperture, reference (monopole mode) signal output, common mode suppression, SCRF certification, and acceptable physical dimensions(<230 mm outer diameter). To simplify the RF read-out electronics, the dipole and monopole mode frequencies were chosen “symmetric” to  $f_{RF}=1.3$  GHz:  $f_{110}=1.46$  GHz,  $f_{010}=1.14$  GHz.

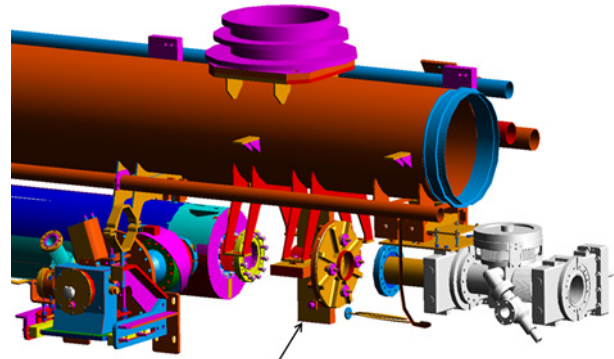


Figure 13: ILC cryomodule with cavity BPM

The Project X bunch structure within the macropulse differs substantially from the ILC, bunches are basically spaced by 1/325 MHz, and no single bunch BPM measurement is required. In this case almost no beam harmonics are present at  $f_{110}=1.46$  GHz, therefore a modified cavity BPM design is underway, working at a dipole mode frequency of  $f_{110}=1.3$  GHz. The Q-factor will stay at 600-700 to perform beam tests at the NML test facility with either Project X multibunch pulses or an ILC-like beam structure based on a large spacing between bunches.

Figure 14(a) shows the designed cold cavity BPM that consists of a 78 mm diameter beam tube, 230 mm diameter cylindrical cavity and rectangular cavity with 60 mm length. The concept of combined cavities on the beam pipe is intended to use high pressure water rinsing inside both cavities to avoid contamination flow into SC cavities. The dimension of the rectangular cavity are chosen for all field modes in rectangular cavity to leak into the beam tube but for edged dipole mode field from cylindrical cavity to be coupled [23]. Therefore, the operating frequency of dipole mode for cold cavity BPM is affected by rectangular cavity length as well as cylindrical cavity diameter. The frequency change along rectangular cavity length is shown in Fig. 14(b). Since a 230 mm cavity diameter is the maximum dimension which can be accommodated, the rectangular cavity length is chosen to satisfy 1.3 GHz operating frequency in the figure. Furthermore, the 1.4 GHz quadrupole mode can be easily rejected with a band pass filter.

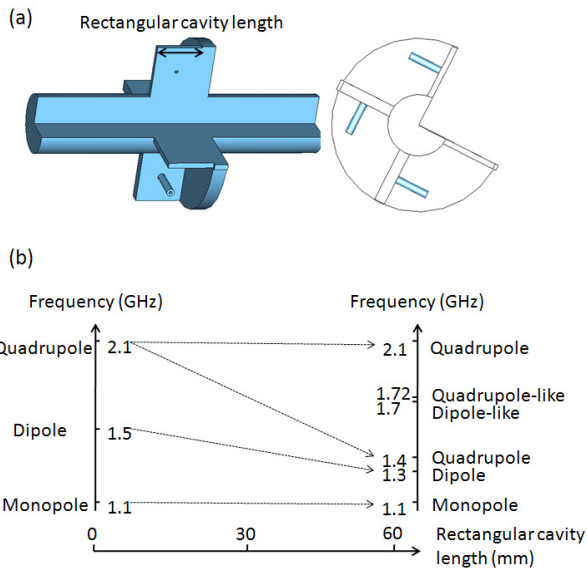


Figure 14: (a) Cavity BPM for Project X / ILC / NML  
(b) Mode classification along rectangular cavity length.

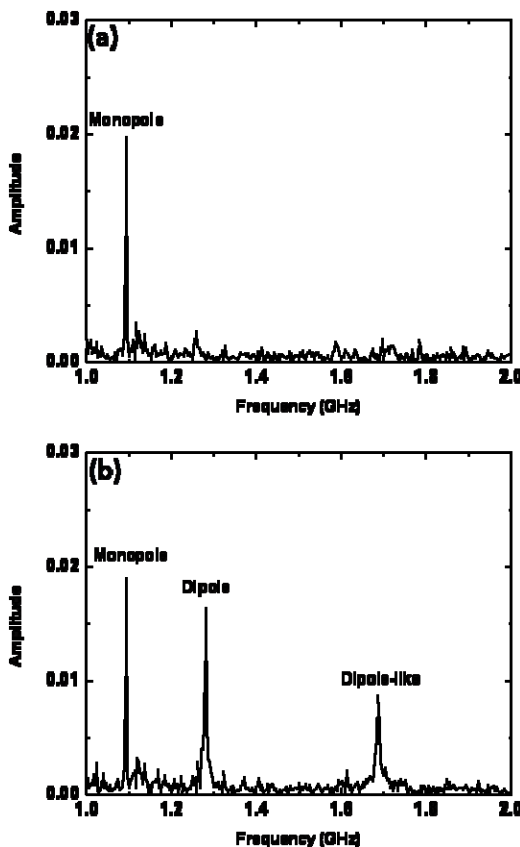


Figure 15: Signal levels at a horizontal (a) and vertical (b) output port.

CST microwave and particle studio are used to design and calculate characteristics for cold cavity BPM. Here CST particle studio is for simulation of moving charged particles in combination with arbitrary time dependent fields. Generated field from passing beam with  $y=1$  mm

offset are recorded on all antenna ports. By the fast Fourier transformation, the recorded output signal is classified into modes in frequency space and the corresponding frequency spectra for each port are shown in Fig. 15. Since beam with only y-offset is considered, dipole mode signal is observed at only y-port in the figure. But monopole mode signals are observed at both ports due to symmetry property of monopole mode. Although monopole mode signal power is considerable, its signal contribution at the dipole mode frequency is low. Therefore an efficient CM-mode rejection, by use of BPF and  $180^\circ$  hybrid combiner, will result in a resolution of 300 nm position signal level for ILC-like beam structure and a few nm position signal level for Project-X like beam structure, respectively (Table 3).

Table 3: Expected cavity BPM signal levels

Condition	Beam:	ILC	Project X
Single bunch dipole, 300 nm offset		200 $\mu$ V	2.8 $\mu$ V
Multibunch dipole, 300 nm offset		200 $\mu$ V	84 $\mu$ V
Single bunch, TM010 contribution		180 $\mu$ V	2.5 $\mu$ V
Multibunch, TM010 contribution		180 $\mu$ V	1.3 $\mu$ V
Single bunch, under 1 $\mu$ rad angle		27 $\mu$ V	0.4 $\mu$ V

### Electron Beam Profile Monitor

When the intensity of a proton beam becomes large enough, conventional profile monitors such as flying wire systems begin to fail due to heating of the wires. Laser wire systems, while not susceptible to beam heating, only work if there is an electron attached to the proton. One alternative to these methods is to use another beam of particles, for instance, using a low energy beam of electrons to measure the profile of a beam of high intensity protons (see Fig. 16). The electron beam originates from an electron gun and travels perpendicular to the proton beam. Typically, there is some sort of deflection mechanism, either electrostatic or magnetic, to step the electron beam through the protons. As it passes through the proton beam it is deflected by the electric fields of the beam dependently on the impact parameter. At the other end of the device, the electron beam is collected by a phosphor screen and/or microchannel plate. The profile can then be obtained from an inverse Radon transform.

This technique has been sporadically in use for at least 40 years. A paper by Stallings [24] in 1971 presented measurements of the charge distribution of a cylindrical column of plasma using an electron beam. In 1987 there was an experiment at TRIUMF to measure the profile of a beam of ions by using the deflection of a 1-2 keV beam of electrons as it was stepped through the ion beam via electrostatic deflection plates [25]. The comparisons with a wire scanner were very promising. In 1993 there was a proposal to use an electron beam at the SSC [26]. At CERN in the late 1990's, an ion beam probe was developed to measure profiles of proton beams at the SPS



and possibly LHC [27]. They tested both a ‘pencil’ beam and a ‘sheet’ beam which could in principle do single shot measurements instead of having to be stepped through the proton beam. Recently, SNS has collaborated with BINP to develop an electron beam profile monitor [28] for use in the SNS accumulator ring (see talk by Assadi at this conference for the first results).

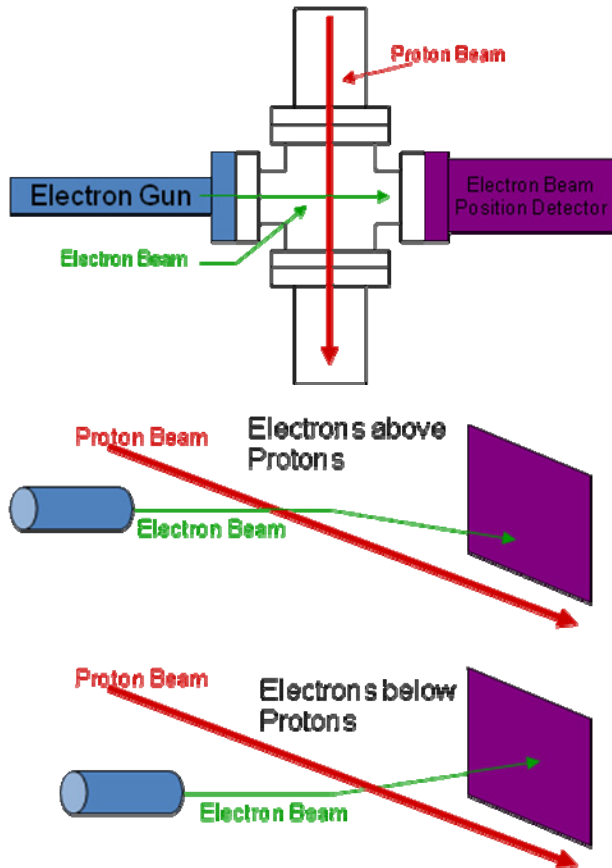


Figure 16: Above the beam, electrons are deflected down and below the beam they are deflected up. In between, their deflection is a function of the charge distribution of the beam.

The main advantages to type of device is that there are no moving parts, there is no danger of damage from the beam, and it is essentially non-destructive. The energy and intensity of the electron gun must be matched to the energy and intensity of the beam to be measured. Fortunately, electron guns in a wide range of capabilities can be easily found.

#### Other Beam Instrumentation Needs

Beside the above examples, several other beam instrumentation and diagnostic techniques have to be considered to meet the requirements in the upcoming high-intensity hadron beam projects at Fermilab, e.g.:

- **Beam Position and Orbit**  
An automatic calibration and gain correction system is required to correct for gain drifts due to temperature and aging effects, to meet the

stringent needs as orbit qualifier in the machine protection systems.

- **Beam Halo Characterization**

Various methods have to be studied to characterize transverse beam halo, e.g. by crawling wire, vibrating wire, or laser wire beam monitors. Also a beam core subtraction method on OTR images, utilizing micro-mirrors, has the potential of increasing the required dynamic range up to  $1:10^5$ .

- **Beam Emittance at Low Energies**

A rotatable *Allison* scanner [29] has the potential to measure beam displacement and divergence at low beam energies in both planes.

- **Longitudinal Beam Properties**

Beam phase monitors are required, as well as the investigation of particle population in the bucket tails. SNS studies a longitudinal beam profile monitor at low energies, based on a ps mode-locked H laser wire.

## REFERENCES

- [1] R. Webber, “Overview and Status of the Fermilab High Intensity Neutrino R&D Program,” this workshop.
- [2] G. Apollinari, “Project X as a Way to Intensity Frontier Physics,” this workshop.
- [3] D. Johnson, “Challenges Associated with 8 GeV H<sup>-</sup> Transport and Injection for Fermilab Project X,” this workshop.
- [4] J. Zagel, et al., “Complementary Methods of Transverse Emittance Measurement,” BIW’08, Lake Tahoe, CA, USA, May 2008, TUPTPF069, to be published.
- [5] A. Jansson, et al., “Ionization Profile Monitoring at the Tevatron,” EPAC’06, Edinburgh, Scotland, June 2006, THYFI01, p. 2777 (2006); <http://www.JACoW.org>.
- [6] Z. Pavlovic, et al., “Segmented Foil SEM Grids for High-Intensity Proton Beams at Fermilab,” DPAC’07, Venice, Italy, May 2007, WEPC27, to be published.
- [7] J. Bossert, J. Mann, G. Ferioli and L. Wartski, “Optical Transition Radiation Proton Beam Profile Monitor,” CERN/SPS 84-17.
- [8] L. Wartski, J. Marcou and S. Roland, “Detection of Optical Transition Radiation and its Application to Beam Diagnostics,” IEEE Trans. Nucl. Sci., vol. 20, no. 3, pp. 544-548 (1973).
- [9] D. W. Rule et al., “The Effect of Detector Bandwidth on Microbunch Length Measurements made with Coherent Transition Radiation,” Advanced Accelerator Concepts: Eighth Workshop, W. Lawson, C. Bellamy, and D. Brosius, eds., AIP 472, p.745-754, 1999.
- [10] C. Fischer, “Results with LHC Beam Instrumentation Prototypes,” DIPAC’01, Grenoble, France, May 2001, IT05, p. 21 (2001); <http://www.JACoW.org>.

- [11] V. E. Scarpine, A. H. Lumpkin, W. Schappert and G. R. Tassotto, "Optical Transition Radiation Imaging of Intense Proton Beams at FNAL," IEEE Trans. Nucl. Sci. **51**, 1529-1532 (2004).
- [12] V. E. Scarpine, A. H. Lumpkin and G. R. Tassotto, "Initial OTR Measurements of 150 GeV Protons in the Tevatron at FNAL," BIW'06, Batavia, IL, USA, May 2006, AIP Conf. Proc 868, p. 473.
- [13] G. R. Tassotto, V. E. Scarpine, A. H. Lumpkin and R. M. Thurman-Keup, "Optical Transition Radiation Imaging of 120 GeV Protons Used for Antiproton Production at FNAL," presented at the 2006 IEEE Nucl. Sci. Symp., San Diego, CA.
- [14] V. E. Scarpine, G. R. Tassotto and A. H. Lumpkin, "OTR Imaging of Intense 120 GeV Protons in the NuMI Beamline at FNAL," PAC'07, Albuquerque, NM, USA, pp. 2639-2641 (2007)
- [15] V. E. Scarpine, C. Lindenmeyer, A. H. Lumpkin and G. R. Tassotto, "Development of an Optical Transition Radiation Detector for Profile Monitoring of Antiproton and Proton Beams at FNAL," PAC'05, Knoxville, TN, USA, pp. 2381-2383 (2005).
- [16] R. Shafer, "Comments on the Tevatron Beam Loss Monitor (BLM) System," Fermilab, Accelerator Division Internal Document, Beams-Doc-790-v1, August 2003.
- [17] R. Connolly, "Laser Profile measurements of an H<sup>-</sup> Beam," PAC'01, Chicago, IL, USA, June 2001, TPAH034, p. 1300 (2001); <http://www.JACoW.org>.
- [18] S. Assadi, "SNS Transverse and Longitudinal Laser Profile Monitors Design, Implementation and Results," EPAC'06, Edinburgh, Scotland, June 2006, THPCH156, p. 3161 (2006); <http://www.JACoW.org>.
- [19] Y. Liu, "Laser Wire Beam Profile Monitor at SNS," EPAC'08, Genoa, Italy. June 2008, TUPC061, p. 1197 (2008); <http://www.JACoW.org>.
- [20] R. Connolly, "A Real-Time Longitudinal Phase-Space Measurement Technique for H<sup>-</sup> Beams," PAC'91, San Francisco, CA, USA, May 1991, p. 1237 (1991).
- [21] R. E. Shafer, "Laser Diagnostics for High Current H<sup>-</sup> Beams," BIW'98, Palo Alto, CA, USA, May 1998, A.I.P. Conf. Proceedings, (451) 191.
- [22] A. Lunin, et al., "Design of a Submicron Resolution Cavity BPM for the ILC Main Linac," DPAC'07, Venice, Italy, May 2007, TUPC23, to be published.
- [23] S. Shin, private communications.
- [24] C.H. Stallings, "Electron Beam as a Method of Finding the Potential Distribution in a Cylindrically Symmetric Plasma," J. Appl. Phys. **42** (1971) 2831.
- [25] V. Shestak, et al., "Electron Beam Probe for Ion Beam Diagnostics," TRIUMF Design Note, TRI-DN-87-36 (1987).
- [26] E. Tsyganov, et al., "Electron Beam Emittance Monitor for the SSC," PAC'93, p. 2489.
- [27] J. Bossert, et al., "Ion Curtain Profilometer," CERN Note CERN-PS-BD-99-15 (1999).
- [28] A. Aleksandrov, et al., "Feasibility Study of Using an Electron Beam for Profile Measurements in the SNS Accumulator Ring," PAC'05, p. 2588.
- [29] P. W. Allison, J. D. Sherman and D. B. Holtkamp, IEEE Trans. Nucl. Sci. NS-30, 2204-2206 (1983).